Vol. **107** (2005) *ACTA PHYSICA POLONICA A* No. 1

Proceedings of the 12th International Symposium UFPS, Vilnius, Lithuania 2004

Small and Large Signal Analysis of Terahertz Generation from InN n^+nn^+ Structures with Free-Carrier Grating

V. Gružinskis, P. Shiktorov and E. Starikov

Semiconductor Physics Institute, A. Goštauto 11, 01108 Vilnius, Lithuania

Electron transport in long (up to 15 μm) InN n^+nn^+ structures is theoretically investigated by the Monte Carlo particle technique at low lattice temperatures when optical phonon emission is the dominating scattering mechanism. It is shown that at constant bias a free-carrier grating can be formed inside the n-region. Such a grating is found to be responsible for microwave power generation in the THz frequency range. The generation mechanism is similar to that in submicron n^+nn^+ structures under quasi-ballistic transport conditions.

PACS numbers: 72.20.Ht, 72.30.+q

1. Introduction

During the last decades, significant efforts were devoted to search of semiconductor sources of tunable terahertz (THz) radiation due to the large interest in their possible applications in broadband communication, high-resolution spectroscopy, and radars, etc. A considerable progress in the growth of nitrides during last five years gives the materials, such as GaN, InN and AlN, of good quality for electronic devices. The main advantages of nitrides as compared with the standard $A^{III}B^{V}$ semiconductors are their higher optical phonon energy and much higher optical phonon emission rate, which are favourable for THz generation realization. Recently a number of publications have appeared on THz radiation possibility in bulk nitrides at low temperatures, when optical phonon emission rate considerably exceeds the scattering rate by all other mechanisms (see [1] and references therein). In bulk materials, a dynamic negative differential mobility can arise due to the cyclic motion of electrons within the optical phonon sphere in momentum space when a constant electric field is applied to the semiconductor. Also the possibility of THz generation in InN n^+nn^+ submicron structures is reported [2]. The generation mechanism predicted by Ryzhij et al. [3, 4] is based on excitation

of coherent electron plasma oscillations by optical phonon emission process under near ballistic electron motion in n-region of the structure.

In this report we consider the submicron and long (up to 15 μm) n^+nn^+ InN structures. In long structures electron transport is close to that of the bulk semiconductor but the spatial dependence of the electric field is accounted for, so that the coexistence of the above two effects can be possible. The calculation of electron transport in n^+nn^+ InN structures is performed through the simultaneous solution of the coupled Boltzmann and Poisson equations by Monte Carlo particle (MCP) technique [5]. The wurtzite InN nonparabolic conduction band structure and the material parameters are taken from [6]. Electron scattering by polar optical phonons, acoustic deformation and piezoelectric phonons, and ionized impurities are accounted for. The piezoelectric constant values are taken from [7]. Due to a relatively high electron heating up to energies of $100 \approx 150$ meV the acoustic scattering is considered to be elastic. The doping of the simulated $0.02{-}L{-}0.02$ μm n^+nn^+ InN structures is $n = 0.2{-}4 \times 10^{16}$ cm^{-3} and $n^+ = 10^{18}$ cm^{-3}. All the calculations are performed for applied voltages $U = 0.152$–6 V with the n-region lengths $L = 0.38{-}15$ μm. The number of simulated particles, depending on the case, varies between 2×10^4 and 10^6. The time step of the Poisson solver in all cases is of 1 fs.

2. Results and discussion

Figure 1a,b shows the formation of a free-carrier grating in real space due to the periodic motion of electrons under optical phonon emission in the n-region at $T = 80$ K. Indeed, a low energy electron injected from the cathode contact is accelerated by the field up to the optical phonon energy and then it loses energy and velocity after optical phonon emission. This process is repeated until the electron leaves the n-region through the anode contact. As a consequence, the electron trajectory consists of a sequence of free flight and stop regions. The stop regions coincide with a maximum of carrier concentration, and their number is an integer part of $eU/\hbar\omega_0$, where e is the electron charge and $\hbar\omega_0$ the optical phonon energy. The spatial dependence of the free carrier concentration (as well as of the field $E(x)$, velocity $v(x)$, energy $\varepsilon(x)$, etc.) is found to become nearly periodic when the doping level N exceeds some critical value $N_{\rm cr}$ (see Fig. 1a, curves 3–5). Therefore, we observe the formation of a free-carrier grating with period $l_0 = \hbar\omega_0/e\overline{E}$, where $\overline{E} \approx U/L$ is the average field in the grating. The electron transport within one grating period can be considered as a transport in a n^+nn^+ structure with l_0 being the length of the n-region, since the stop region serves as cathode and anode contact at the same time. It is well known [8] that under pure ballistic conditions all the field in the l long n^+nn^+ structure is concentrated in a small region of length $l_{\rm u}$ near the cathode contact so that in the remaining n-region the field is zero at $l > l_{\rm u} = \pi\sqrt{\kappa\kappa_0 U/2eN}$, where κ is the

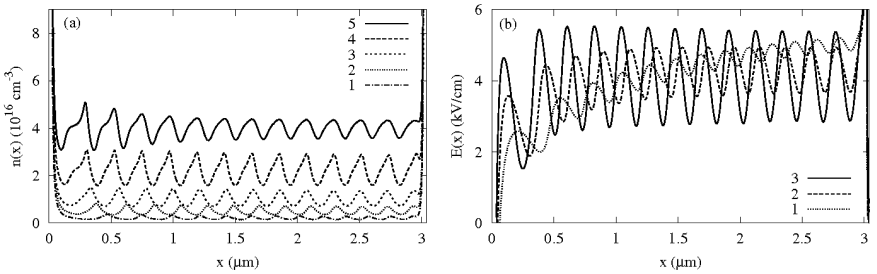

Fig. 1. Concentration (a) and electric field (b) profiles in the n-region of an n^+nn^+ InN structure at 80 K, 1.2 V bias and different dopings N of the n-region: curves from 1 to 5 correspond to $N = 0.2$, 0.5, 1, 2.2, and 4×10^{16} cm^{-3}.

electric permittivity, $\kappa_0 = 8.85 \times 10^{-12}$ F/m, and N the doping of the n-region. A periodic grating can be created by optical phonon emission, when $l_0 > l_u$. This condition gives the criterium for minimal doping: $N_{cr} = \kappa\kappa_0(\pi U/L)^2/2\hbar\omega_0$. For the InN structure under study $N_{cr} = 7.5 \times 10^{15}$ cm^{-3}. For the case of an l_0 long n^+nn^+ InN structure at a bias $u_0 = \hbar\omega_0/e$, which corresponds to one grating period, N_{cr} is the threshold doping for the onset of a plasma instability in the structure under quasiballistic transport conditions [2–4].

The linear response of the InN structure is calculated by simulating with the MCP technique the current response to a periodic voltage $U(t) = U_0 + U_1 \cos(2\pi ft)$, where f is the frequency, t the time, U_0 the voltage, and $U_1 = 0.1U_0$. Figure 2 reports the frequency behaviour of the real parts of the admittance $\mathrm{Re}\{Y(f)\}$ for submicron $L = 0.38$ μm (a) and long $L = 3$ μm (b) InN structures depending on n-region doping at $T = 10$ K. The applied voltages of $U_0 = 0.152$ V to the submicron structure and $U_0 = 1.2$ V to the long one are chosen to give the same $N_{cr} = 7.5 \times 10^{15}$ cm^{-3} value for both structures. The behaviour of $\mathrm{Re}\{Y(f)\}$ dependence on doping of submicron InN structure (Fig. 2a) is close to that calculated analytically for quasiballistic transport conditions in submicron diode structures [3, 4]. The sharp increase in negative $\mathrm{Re}\{Y(f)\}$ values with

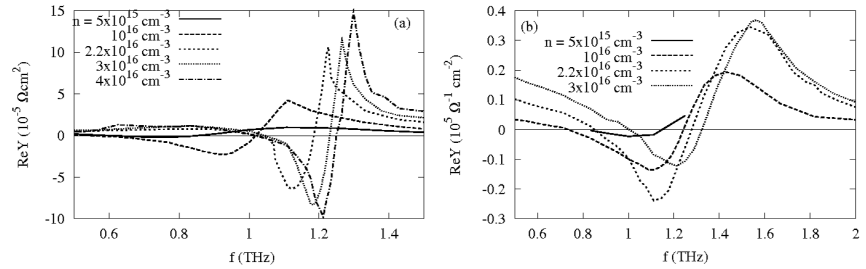

Fig. 2. Real part of admittance $\mathrm{Re}\{Y(f)\}$ for submicron $L = 0.38$ μm (a) and long $L = 3$ μm (b) InN structures as a function of n-region doping at $T = 10$ K and applied voltages: $U_0 = 0.152$ V to the submicron structure and $U_0 = 1.2$ V to the long structure.

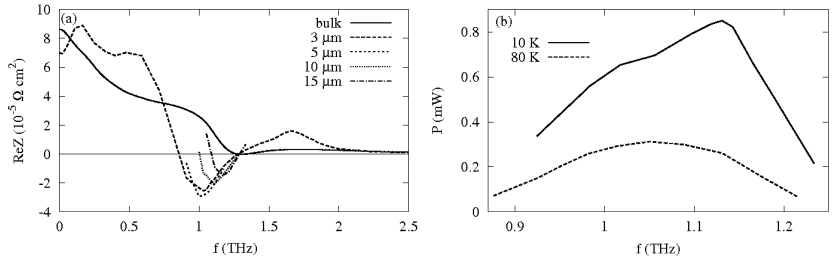

Fig. 3. Real part of impedance $\mathrm{Re}\{Z(f)\}$ for long InN structures (a) as a function of n-region length at $T = 10$ K, $N = 2.2 \times 10^{16}$ cm^{-3}, and $U_0/L = 4$ kV/cm. For comparison the impedance for 3 μm long structure recalculated from the bulk differential mobility data is also shown. Part (b) shows generated power spectra of 3 μm long InN diode with $N = 2.2 \times 10^{16}$ cm^{-3} operating in a parallel resonant circuit at $U_0 = 1.2$ V and 10 and 80 K.

increased doping at $N > N_{\mathrm{cr}}$ is observed for submicron structures. The same feature is typical of the long structures (see Fig. 2b). Also in both cases the frequency range of negative $\mathrm{Re}\{Y(f)\}$ values is shifted to the higher frequencies with increased doping. Therefore the physical mechanism of negative admittance in 3 μm long InN structure is similar to that in submicron structure at quasiballistic transport conditions [3, 4]. On the other hand, in very long InN structures the conditions for negative admittance should approach the conditions for bulk semiconductors. In Fig. 3a the impedances of 3, 5, 10, and 15 μm long InN structures at $T = 10$ K are shown. The doping of structures is 2.2×10^{16} cm^{-3} and $U_0 = 1.2$, 2, 4, and 6 V, respectively. For comparison, Fig. 3a also reports the small signal impedance $Z(f) = [en\mu(f)/L + \mathrm{i}2\pi f C_L]^{-1}$ obtained for the considered diode with length L and geometrical capacitance C_L from the small-signal mobility $\mu(f)$ calculated by MC simulation of the bulk material [1] subjected to an electric field equal to U/L in the n-region (i.e. without the grating). The $\mathrm{Re}Z(f)$ is recalculated for 3 μm long InN structure. The comparison of the recalculated from bulk mobility and directly simulated by MCP $\mathrm{Re}Z(f)$ of 3 μm long InN structures shows the more or less good agreement between impedances at low and high frequencies. The difference between the characteristics at intermediate frequencies is rather essential. The main difference is in the frequency range and amplitude of negative $\mathrm{Re}Z(f)$ values. The MCP simulation results on longer than 3 μm InN structures show as expected the approach of the main $\mathrm{Re}Z(f)$ characteristic to the bulk case at increased L. Therefore, the bulk effect is responsible for the negative values of impedance in the sufficiently long (about of several tens of μm) structures.

The microwave power generation from the long InN structure operating in a parallel resonant circuit is simulated. A standard 50 Ω load resistor and a 0.005 pH inductor are connected in parallel with a variable capacitor and then in series with the structure. The generation frequency is tuned by the capacitor. The

cross-sectional area of the structure is assumed to be 4000 μm^2. The frequency dependence of the microwave power generated by the simulated InN diode connected in parallel with the resonant circuit is reported in Fig. 3b. The parameters of simulated structure are $L = 3$ μm, $N = 2.2\times10^{16}$ cm^{-3}, and $U = 1.2$ V. The microwave generation is simulated at temperatures of 10 K and 80 K. As expected, microwave power is generated in the frequency region, where $\mathrm{Re}\{Z(f)\}$ is negative (compare $\mathrm{Re}\{Z(f)\}$ of Fig. 3a with curve at 10 K of Fig. 3b). In addition, Fig. 3b shows that at 10 K the generated power considerably exceeds that generated at 80 K. The reason of this behaviour stems from the fact that as temperature increases the scattering by deformation and piezoelectric acoustic phonons grows and, as a result, deteriorates the time-periodicity of optical phonon emission. Moreover, such increased scattering efficiency leads to a decrease in electron velocity and transit-time frequency f_0, which is proportional to the velocity. As a result, the microwave power generation maximum at 80 K appears at a frequency which is lower than that at 10 K. Also MCP simulation shows the generated power decrease with temperature increased. Therefore, at given frequency 1.09 THz with temperature increased from 30 to 120 K the generated power decreases from 0.737 to 0.063 mW.

The MCP analysis of the evolution of the space charge profile during microwave power generation in the resonant circuit does not show the creation of any travelling structures like domains or accumulation layers inside the n-region of the InN diode. Therefore, the generation frequency does not depend on the length L of the n-region as in the Gunn or IMPATT diodes.

Another typical feature of microwave power generation in structures with grating is the resonant-like dependence of the generated power at a given frequency on the n-region doping. As MCP simulations of InN structures shows, at conditions corresponding to $f_0 = 0.2$–1.4 THz, the maximum generated power is extracted when f_0 coincides with the plasma frequency $\omega_\mathrm{p}/2\pi$ defined as $\omega_\mathrm{p} = \sqrt{e^2 n/\kappa\kappa_0 m^*}$, where n is the electron density of the plasma and m^* is electron effective mass. By recalling that in the considered InN structure $n = N$, the above condition gives the optimal doping N_op for maximum generated power in frequency range around f_0: $N_\mathrm{op} = \kappa\kappa_0 m^*(2\pi\overline{E}\overline{v}/\hbar\omega_0)^2$. For the considered InN structure with grating $N_\mathrm{op} = 2.2\times10^{16}$ cm^{-3}.

3. Conclusions

In conclusion, we have shown the possibility of realization of a free-carrier grating in long (few μm) InN n^+nn^+ structures at constant bias and low temperatures, when the dominant scattering mechanism is optical phonon emission. In such conditions, InN n^+nn^+ diodes can generate microwave power which can be used for the development of radiation sources in the THz frequency range. As shown by our preliminary MCP simulations the same effect is possible in other

nitrides as GaN and AlN and $A^{III}B^{V}$ semiconductors. In the latter case the generation frequency is well below the THz frequency range because of a much weaker scattering by optical phonons as compared with nitrides.

References

[1] E. Starikov, P. Shiktorov, V. Gružinskis, L. Reggiani, L. Varani, J.C. Vaissière, J.H. Zhao, *J. Phys., Condens. Matter* **13**, 7159 (2001).

[2] E. Starikov, V. Gružinskis, P. Shiktorov, *Phys. Status Solidi A* **190**, 287 (2002).

[3] N.A. Bannov, V.I. Ryzhij, V.A. Fedirko, *Pis'ma ZhETF* **7**, 1118 (1981).

[4] V.I. Ryzhij, N.A. Bannov, V.A. Fedirko, *Fiz. Tekh. Poluprovodn.* **18**, 769 (1984).

[5] V. Mitin, V. Gružinskis, E. Starikov, P. Shiktorov, *J. Appl. Phys.* **75**, 935 (1994).

[6] B.E. Foutz, S.K. O'Leary, M.S. Shur, L.F. Eastman, *J. Appl. Phys.* **85**, 7727 (1999).

[7] F. Bernardini, V. Fiorentini, D. Vanderbilt, *Phys. Rev. B* **63**, 193201 (2001).

[8] M.S. Shur, L.F. Eastman, *IEEE Trans. Electron. Devices* **ED-26**, 1677 (1979).